# REPORT DOCUMENTATION PAGE

AFRL-SR-AR-TR-04-

0158

| 1. REPORT DATE (DD-MM-YYYY) 12-31-2003 | 2. REPORT TYPE Final Report | 3. DATES COVERED 8/1/03-12/31/03 |
|---|---|---|

| 4. TITLE AND SUBTITLE Optimization of Off-Axis ICOS and Applications to Flow Tube Kinetics | 5a. CONTRACT NUMBER F49620-03-1-0412 |
|---|---|
| | 5b. GRANT NUMBER |
| | 5c. PROGRAM ELEMENT NUMBER |

| 6. AUTHOR(S) Manish Gupta and Anthony O'Keefe | 5d. PROJECT NUMBER |
|---|---|
| | 5e. TASK NUMBER |
| | 5f. WORK UNIT NUMBER |

| 7. PERFORMING ORGANIZATION NAME(S) AND ADDRESS(ES) Los Gatos Research 67 East Evelyn Avenue Suite 3 Mountain View, CA 94041 | 8. PERFORMING ORGANIZATION REPORT NUMBER 4081 |
|---|---|

| 9. SPONSORING / MONITORING AGENCY NAME(S) AND ADDRESS(ES) USAF, AFRL AF Office of Scientific Research 4015 Wilson Blvd, Room 713 Arlington, VA 22203-1954 | 10. SPONSOR/MONITOR'S ACRONYM(S) AFOSR |
|---|---|
| | 11. SPONSOR/MONITOR'S REPORT NUMBER(S) |

**12. DISTRIBUTION / AVAILABILITY STATEMENT**

Approve For Public Release: Distribution Unlimited.

**13. SUPPLEMENTARY NOTES**

**14. ABSTRACT**

In this AFOSR granting period, Los Gatos Research explored the capabilities of Off-Axis Integrated Cavity Output Spectroscopy (Off-Axis ICOS) with an especial emphasis towards flow-tube kinetics studies. Specifically, research was performed to ascertain the application of Off-Axis ICOS to spatial imaging, time-dependant phenomenon, and through-plasma spectroscopy. Achievements included developing a theoretical framework to simulate spot pattern images in the presence of spatially-inhomogeneous cavity loss, simulating the time-dependent cavity transmission for both impulse function and rapidly-modulating absorption losses, and measuring a variety of energetic species within a radio frequency inductively coupled plasma (RF-ICP).

## 20040319 112

| 15. SUBJECT TERMS Off-Axis ICOS, Flow Tube Kinetics | | | | | |
|---|---|---|---|---|---|

| 16. SECURITY CLASSIFICATION OF: | | | 17. LIMITATION OF ABSTRACT | 18. NUMBER OF PAGES | 19a. NAME OF RESPONSIBLE PERSON Manish Gupta |
|---|---|---|---|---|---|
| a. REPORT Unclassified | b. ABSTRACT Unclassified | c. THIS PAGE Unclassified | | 11 | 19b. TELEPHONE NUMBER (include area code) 650-965-7874 |

Standard Form 298 (Rev. 8-98)
Prescribed by ANSI Std. Z39.18

# Final Report

# Optimization of OA-ICOS and Applications to Flow Tube Kinetic Studies

Dr. Manish Gupta
Dr. Anthony O'Keefe
Los Gatos Research
67 East Evelyn Avenue, Suite 3
Mountain View, CA 94043
(650) 965-7772

# Overview

The object of this AFOSR-funded research effort was to further explore the capabilities of Off-Axis Integrated Cavity Output Spectroscopy (Off-Axis ICOS) with an especial emphasis towards flow-tube kinetics studies. Specifically, research was performed to ascertain the application of Off-Axis ICOS to spatial imaging, time-dependant phenomenon, and through-plasma spectroscopy. Achievements included developing a theoretical framework to simulate spot pattern images in the presence of spatially-inhomogeneous cavity loss, simulating the time-dependent cavity transmission for both impulse function and rapidly-modulating absorption losses, and measuring a variety of energetic species within a radio frequency inductively coupled plasma (RF-ICP).

# Spatial Imaging

In Off-Axis ICOS, a cw-laser is inserted into a high-finesse optical cavity in an off-axis fashion (the input beam is displaced from the cavity center). The beam then traces a complex pattern that depends on the mirror reflectivity, mirror radius of curvature, and off-axis alignment. Three measured images are shown in Figure 1. The leftmost corresponds to an on-axis alignment and represents the beam bouncing back and forth upon itself. The middle image is obtained when the laser is moved vertically off-axis but no tilt is imparted to the beam. Note that this configuration may be particularly well-suited for flow tube studies, in which a narrow detection zone along the flow axis permits fast time resolution. The rightmost image results when the beam is both moved off-axis and tilted. Although a circular pattern is to be expected, a square pattern results due to the astigmatism of the mirrors (probably due to imperfect polishing and stress induced during coating). In Off-Axis ICOS, the most sensitive absorption measurements occur when the beam overlaps the least upon itself (smallest opportunity to interfere with itself), and thus the rightmost image provides the best absorption sensitivity.
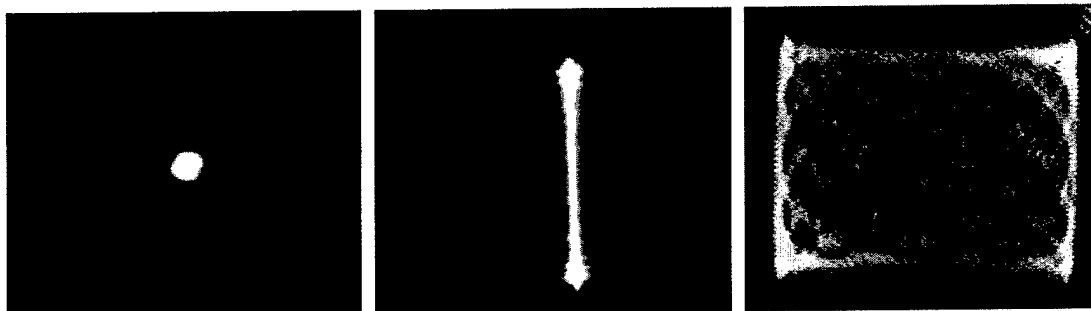


**Figure 1:** Typical spot patterns observed through the rear cavity mirror. The specific pattern can be varied between on-axis (leftmost), straight line (center), and complex Lissajious (rightmost) by changing the input alignment. Note that, were the mirrors perfectly spherical, the rightmost pattern would be circular (or elliptical).

# Theory

The spatial patterns observed through the cavity can be accurately modeled by using simple ray tracing methods detailed by Herriot in 1965. These methods involve starting

with an initial condition vector, $r_0 = (x_0, S_x, y_0, S_y)$, that consists of off-axis positions ($x_0$, $y_0$) and input tilt ($S_x$, $S_y$). This vector is then multiplied by a transmission matrix, $T_L$

$$T_L = \begin{matrix} 1 & L & 0 & 0 \\ 0 & 1 & 0 & 0 \\ 0 & 0 & 1 & L \\ 0 & 0 & 0 & 1 \end{matrix}$$

where L is the cavity length. This matrix results in a vector, **r**, that specifies a point (x,y) on the back mirror. The beam is then reflected off the mirror by multiplying by a matrix, $T_R$

$$T_R = \begin{matrix} 1 & 0 & 0 & 0 \\ -2/a_1 R & 1 & 0 & 0 \\ 0 & 0 & 1 & 0 \\ 0 & 0 & -2/a_2 R & 1 \end{matrix}$$

where R is the mirror radius of curvature and a is the mirror astigmatism (with the subscript referring to a particular axis). In order to translate the beam back onto the front mirror (input mirror), the vector, **r**, is again multiplied by $T_L$. The position vector after the nth bounce is thus given by

$$r_n = (T_R T_L)^n r_0$$

Note that odd bounces (n = 1, 3, 5 ...) correspond to positions on the back mirror and even bounces (r = 0, 2, 4 ...) correspond to positions on the front (input) mirror. The intensity of the nth bounce, $I_n$, relative to the n-1 bounce, $I_{n-1}$ is given by

$$I_n = (R - A)I_{n-1}$$

where R is the mirror reflectivity and A is the per pass absorption for that particular trajectory (assuming a spatially dependent loss function). For a typical mirror reflectivity of 99.99% and no absorption loss, after 10000 bounces, the intensity is still 37% of its original value.

## Simulations

The above equations were programmed into IGOR (Wavemetrics Incorporated) and various simulations were performed to better assess the possibility of using Off-Axis ICOS to measure spatially inhomogeneous losses. Three such simulated patterns are shown in Figure 2, corresponding to on-axis, off-axis with no tilt, and off-axis with tilt (and astigmatism) alignments. Note that the predicted patterns closely match the observed ones shown in Figure 1 as expected.
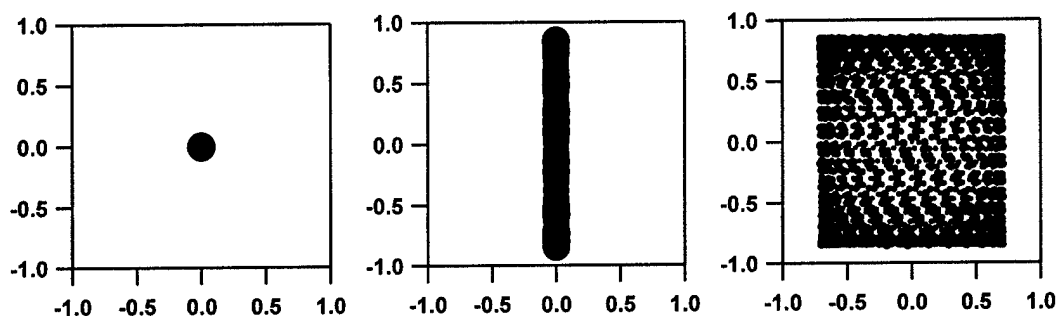
**Figure 2:** Simulated spot patterns for a 22 cm long cavity consisting of two astigmatic mirrors ($R_1$ = 100 cm, $R_2$ = 99.1 cm). The launch conditions were changed from on-axis (leftmost, $x_0 = 0$, $y_0 = 0$, $S_x = 0$, $S_y = 0$) to line (middle, $x_0 = 0$, $y_0 = -0.8$, $S_x = 0$, $S_y = 0$) to off-axis (rightmost, $x_0 = 0$, $y_0 = -0.8$, $S_x = -0.02$, $S_y = 0$).

## Formation of Patterns

In order to better understand the beam trajectory within the cavity, the simulations can be performed with fewer bounces (but comparable mirror reflectivity). Figure 3 illustrates pattern formation by plotting the first 10, 100, and 1000 bounces for a mildly astigmatic cavity. Note that the beam bounces across the mirror face due to the mirror's radius of curvature and rotates slightly due to the input tilt. The mirror astigmatism keeps the beam from tracing an ellipse by rotating the major/minor axes of the ellipse such that they form a square.
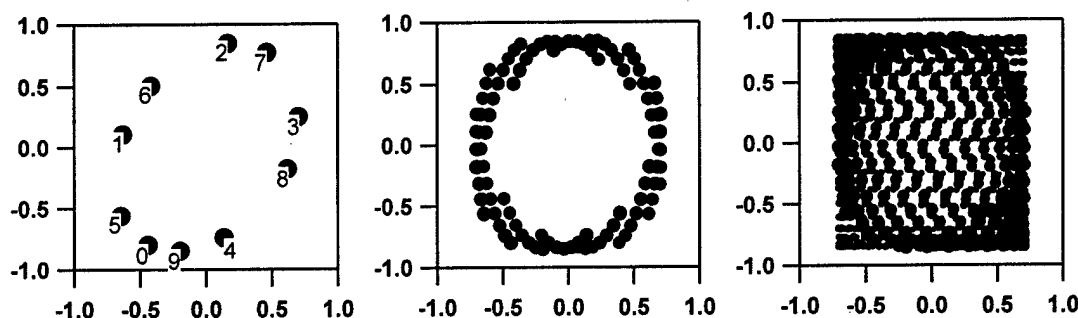
**Figure 3:** Depiction of complex pattern formation for off-axis, astigmatic cavity. The pattern formation is shown after 10, 100, and 1000 bounces with the former bounces numbered for clarity. Note that, for typical Off-Axis ICOS cavities, over 10,000 bounces are observed with only a factor of 2 reduction in intensity.

## Effect of Astigmatism

The effect of mirror astigmatism can best be observed by running a similar set of simulations while changing the astigmatism of the mirrors slowly. Figure 4 shows the result of this simulation. Note that the circular pattern becomes more and more space filling as the mirror astigmatism is increased. This characteristic has been exploited by Off-Axis ICOS to help reduce noise due to optical interferences by deliberately astigmatizing the mirrors.
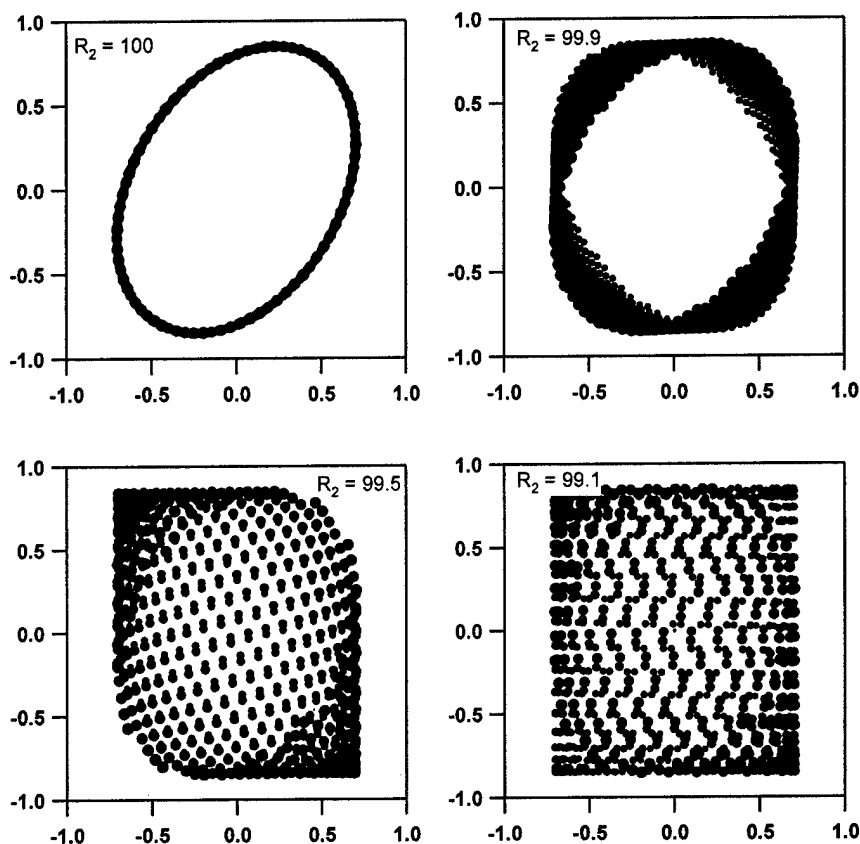
4

**Figure 4:** Simulated spot patterns showing how the mirror astigmatism affects the observed image. For Off-Axis ICOS, the best signal to noise ratio is observed for patterns in which the spot overlap is the least.

## Spatially-Inhomogeneous Loss

One of the key motivations for developing the aforementioned theoretical framework is the possibility of using the complex beam spot pattern to determine the spatial distribution of an absorber. This idea, originally proposed by Dr. Skip Williams at Hanscom Airforce Base, would entail using a high-resolution camera to measure the cavity output pattern and then fitting the pattern to determine the spatial distribution of the absorber (e.g. analogous to an Abel transform). In order to begin assessing the possibility of this intriguing proposal, we have simulated several cavity output spot patterns with various inhomogeneous absorption losses near the back mirror. Note that the patterns are not startlingly different at first appearance. However, since the pattern is mathematically unique, we suspect that a transform to determine loss may be possible, and Dr. Williams intends to pursue this possibility in his laboratory.
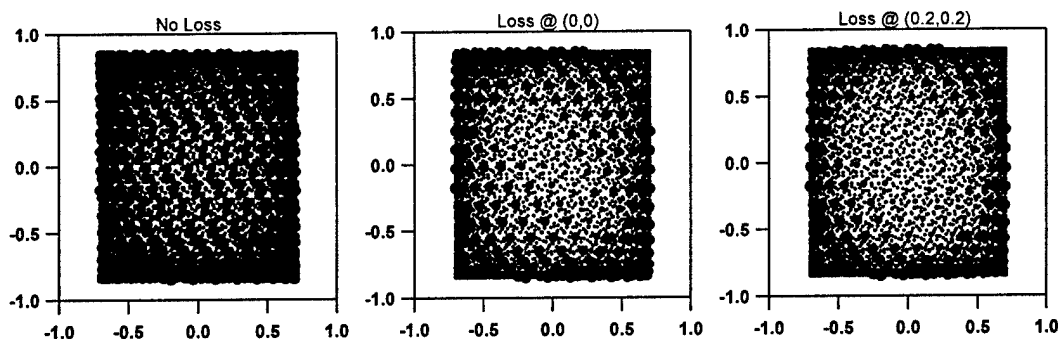
**Figure 5:** Dependence of cavity output spot pattern on spatially inhomogeneous loss within cavity. The loss function is simulated as a 2-d Gaussian function centered at the coordinates listed atop the panels and located at the center of the cavity.

# Time-Dependent Loss Functions

For many Air Force applications, the absorber changes over time. Important examples include fast pulses plasmas in which a species is created virtually instantaneously before exponentially decaying due to chemical reactions and slower pulsed phenomenon in which the species is detected during the pulse. For typical single-pass absorption spectroscopy, the temporal response of the system is dictated by the detector bandwidth (or laser sweep frequency if an absorption feature is being interrogated). In Off-Axis ICOS, the situation is complicated by the fact that light takes a substantial amount of time to pass through the cavity (e.g. for an effective pathlength of 10,000 meters, light takes 33 microseconds to exit the cavity on average).

## Theory

The circulating optical intensity in the cavity is a result of competition between light entering the cavity due to the incident intensity, and light leaving through both mirrors due to finite reflectivity and absorption. The governing differential equation is

$$\frac{dI_{circ}}{dt} = \frac{c}{2L}\left[I_{inc}C_pT - 2I_{circ}\left(1 - Re^{-\alpha L}\right)\right]$$

where

| | | |
|---|---|---|
| $I_{circ}$ | = | Circulating Intensity |
| t | = | time |
| c | = | speed of light |
| L | = | cavity length |
| $I_{inc}$ | = | Incident Intensity |
| $C_p$ | = | coupling constant |
| T | = | mirror transmission |
| R | = | mirror reflectivity |
| $\alpha$ | = | absorbance |

Solving this equation yields

6

$$I_{circ} = \frac{I_{inc} C_P T}{2(1 - Re^{-\alpha L})} \left(1 - e^{-t/\tau}\right)$$

where $\tau$ is the cavity ringdown time and equals

$$\tau = \frac{L}{c(1 - Re^{-\alpha L})}$$

The measured, transmitted intensity, $I_T$, is just this circulating intensity multiplied by the transmission of the rear mirror, T

$$I_T = T I_{circ}$$

Note that the temporal convolution is not as straight forward as just convoluting the cavity output with the ringdown time, because the ringdown time is a function of absorption within the cavity and is thus smaller at the absorption peak. For example, in the extreme case of a very saturated absorber, the ringdown time would approach zero at the absorption peak, whereas it would be much longer in the wings of the feature.

## Simulations

The above temporal convolution was simulated using IGOR to determine its effect on absorption lineshapes, impulse generated absorbers, and pulsed absorption species. Experimental work is expected follow in Dr. Williams' laboratory where time-dependent absorbers can be readily generated.

### Absorption Lineshape

In Off-Axis ICOS, the laser is typically tuned over the absorption feature by rapidly varying its current. In general, the laser is repeatedly tuned over approximately 1 cm⁻¹ (30 GHz) in 0.01 seconds (100 Hz) and the observed transmission spectra are averaged to reduce noise. However, since the cavity the finite time response described above, the lineshape is slightly skewed. This effect is shown for a typical cavity-enhanced absorption trace in Figure 6. The absorption feature has a FWHM of 633 MHz corresponding to about 211 microseconds at the aforementioned sweep rate. For a cavity with a ringdown time of 33.3 microseconds (e.g. 1 meter long, R = 99.99%), the absorption feature is skewed, moving 184 MHz to the right and broadening to approximately 813 MHz. Since the are under the absorption feature is conserved, the peak broadening results in a 8% decrease in the absorption strength. When the skewed absorption is fit to a regular Voigt function, the residual shows the characteristic skewed "Gull-Wing" shape shown in the figure. Note that the amount of skewing depends critically on the tuning rate of the laser versus the cavity ringdown time. For slow tuning rates or fast ringdown times, the skewing will be much smaller, becoming almost unnoticeable. Likewise, if the tuning rate is very fast or ringdown time very long, the lineshape skewing becomes dramatic.
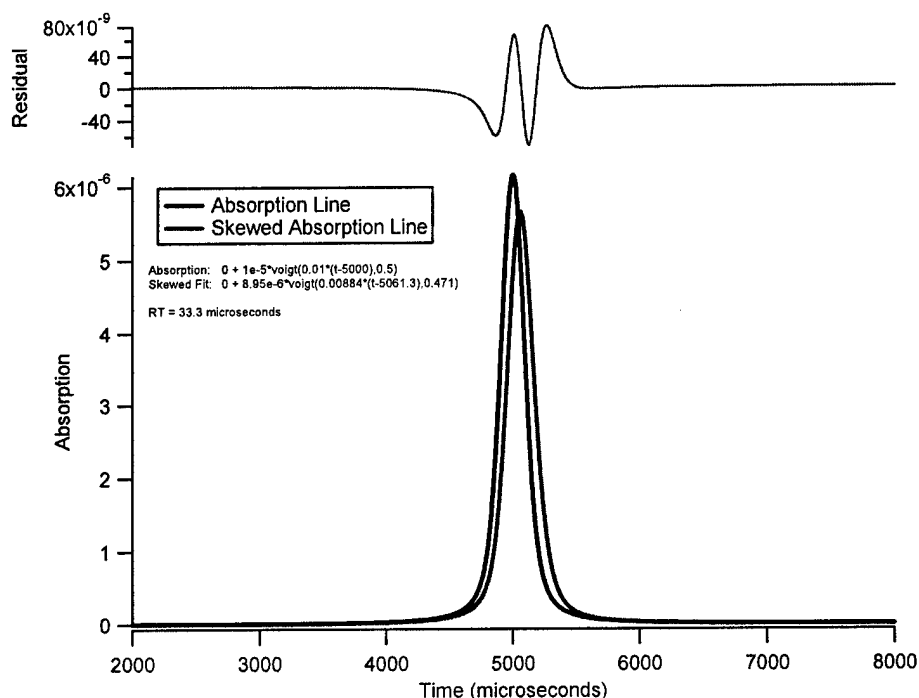
**Figure 6:** Standard absorption feature (blue) skewed by cavity (red) due to finite time response. The skewed feature has been fit to a Voigt function (black), yielding the characteristic asymmetric "Gull-Wing" residual shown atop the figure.

## Time-Dependent Absorptions

In many situations of interest to the Air Force, the absorbing species of interest changes with time. Specific examples include impulse function absorbers, which are generated almost instantaneously (e.g. nanoseconds) and then decay slowly (e.g. microseconds) due to chemical reactions (or radiative decay), and periodically-pulsed plasma species, which only exist during the several microsecond long plasma pulse. In either case, the cavity time response convolutes with the absorbers and the effect must be taken into account.

Figure 7 shows an impulse-generated absorber decaying exponentially with a time constant of 10 microseconds. The cavity output is simulated for several different ringdown times relative to absorption. Note that, in general, the cavity response must be much faster (e.g. 3-6 times) than the change in the absorber if the response time is to be ignored.
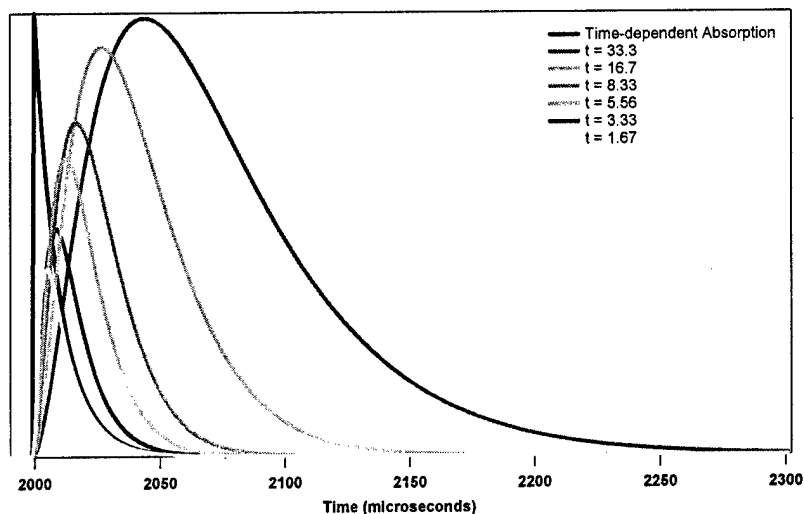
**Figure 7:** Cavity-enhanced absorption for an impulse-generated absorber (black) decaying with a 10 microsecond exponential time constant. The cavity-enhanced signal has been simulated for several different time response cavities.

# Through-Plasma Measurements

The Air Force has long had an interest in energetic species and plasma studies. In this research effort, we have made Off-Axis ICOS measurements through a RF-ICP and detected a variety of highly energetic species (e.g. metastable species and perhaps ions). A variety of plasmas were investigated, including $O_2/He$, $H_2/He$, He, and $N_2$.

**$O_2$/He Plasma**

A 10% $O_2$ in He plasma was investigated near 1524 nm to look for the vibrationally-excited singlet oxygen in the plasma, $O_2$ a$^1\Delta_g$ (v=1). Spectra of both water vapor and plasma species are shown in Figure 8. Note that the central wavelength was determined roughly by a wavemeter and then more exactly by calibrating the water lines relative to the HITRAN database. The observed features did not match the expected singlet oxygen transition frequencies and are therefore probably due to other plasma species.

**$H_2$/He Plasma**

Similar cavity-enhanced absorption spectra were measured through a 6.7% $H_2$ in He plasma in hopes of observing $H_3^+$. The spectrum is shown in Figure 9; however, considerably more effort will be required to assign the observed peaks due to the plethora of possible species in the plasma. Note that both a pure He plasma and ambient water were also measured to confirm that the observed absorption features were due to hydrogen.
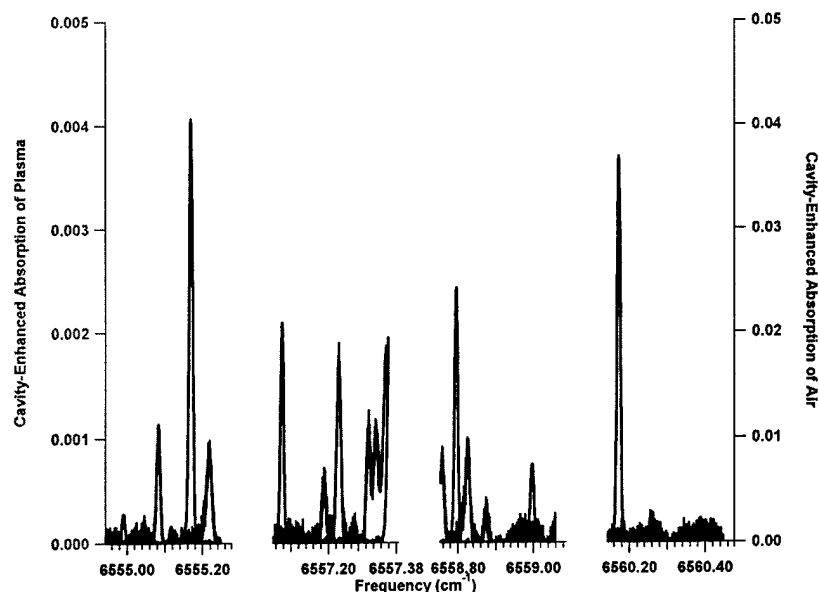
9

**Figure 8:** Measured cavity-enhanced absorption spectra through a 10% oxygen/helium plasma (red) with ambient water absorption features (blue) for spectral calibration. Note that the observed absorption features do not match expected frequencies for vibrationally-excited singlet oxygen, and are therefore likely due to other plasma species.
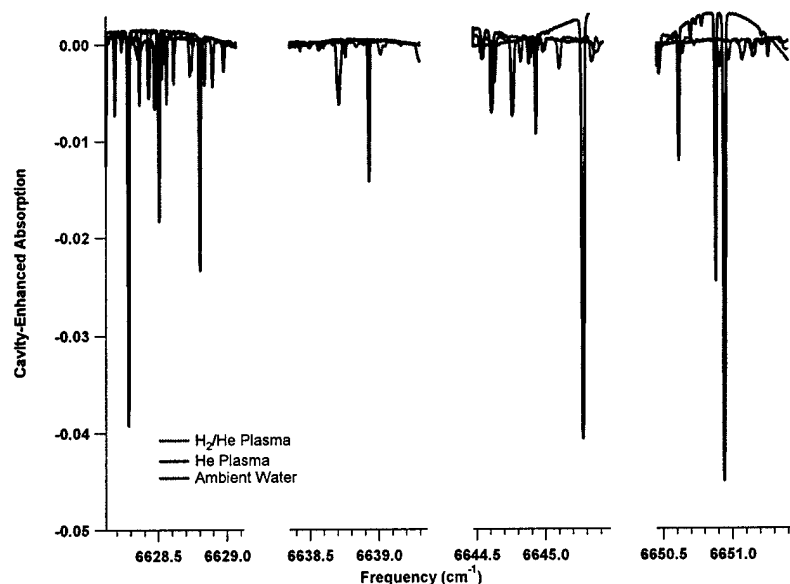


**Figure 9:** Cavity-enhanced absorption spectra through a hydrogen/helium plasma (red). Both pure helium plasma and ambient air spectra were measured for comparison. Note that, due to the very strong water absorptions near this region, some of the ambient air spectra display curved baselines.

## N₂ Plasmas

In hopes of analyzing a simpler system, measurements were taken through N₂ plasmas. However, as depicted in Figures 10, the absorption spectra through these plasmas also consisted of multiple transitions and will require more research to disentangle.
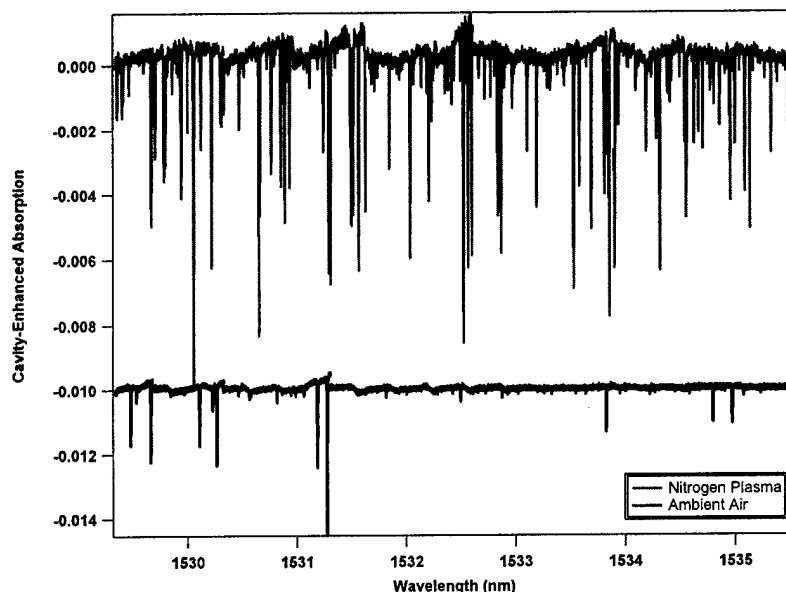
10

**Figure 10:** Measured cavity-enhanced absorption spectrum through a nitrogen RF-ICP (red). A complimentary spectrum of 1.7 torr of ambient room air is included for reference (black) and has been offset by -0.01 absorption units for clarity. Note that, due to the extraordinary number of absorption features, transitions have yet to be identified.

# Future Work

This AFRL-funded research effort clearly shows that Off-Axis ICOS has much promise in a variety of Air Force applications including spatial and temporal imaging for flow tube studies and intra-plasma measurements. Dr. Skip Williams intends to continue the spatial imaging and temporal deconvolution studies in his laboratory at Hanscom Air Force Base. Los Gatos Research intends to pursue continued funding to further study energetic species within plasmas (e.g. metastables and ions). These studies will involve identifying appropriate species of interest to the Air Force, measuring their spectra in a RF-ICP, and accurately identifying the absorption features. We hope to eventually relate these measurements to key plasma parameters such as the Electron Energy Distribution Function and thus provide a direct measurement of plasma operation.

11